Title: **Electrical synapses between inhibitory neurons shape the responses of principal neurons to transient inputs in the thalamus**

Authors: Tuan Pham and Julie S. Haas

Affiliation: Department of Biological Sciences, Lehigh University, Bethlehem, PA

Abstract

As multimodal sensory information proceeds to the cortex, it is intercepted and processed by the nuclei of the thalamus. The main source of inhibition within thalamus is the reticular nucleus (TRN), which collects signals both from thalamocortical relay neurons and from thalamocortical feedback. Within the reticular nucleus, neurons are densely interconnected by connexin36-based gap junctions, known as electrical synapses. Electrical synapses have been shown to coordinate neuronal rhythms, including thalamocortical spindle rhythms, but their role in shaping or modulating transient activity is less understood. We constructed a four-cell model of thalamic relay and TRN neurons, and used it to investigate the impact of electrical synapses on closely timed inputs delivered to thalamic relay cells. We show that the electrical synapses of the TRN assist cortical discrimination of these inputs through effects of truncation, delay or inhibition of thalamic spike trains. We expect that these are principles whereby electrical synapses play similar roles in processing of transient activity in excitatory neurons across the brain.

Introduction

It is well known that thalamocortical (TC) neurons relay sensory information to the cortex. For example, sensory information from rodent whiskers is projected from trigeminal nuclei to the ventroposteromedial (VPM) nuclei and posteromedial (POm) nuclei in the thalamus (Alloway, 2008). From VPM and POm, afferent connections relay information about whisking to the barrels of the primary somatosensory cortex (RRR). Within each of these nuclei, whisker inputs are encoded by varied latencies or spike rates (Sosnik *et al.*, 2001; Yu *et al.*, 2015).

During thalamocortical sensory relay, TC neuronal activity is regulated by a sheet of GABAergic neurons in the thalamic reticular nucleus (TRN)(Houser *et al.*, 1980). Most neurons within the ventrobasal complex (VB) receive monosynaptic GABAergic inputs from TRN neurons, and there is strong monosynaptic excitation from VB to TRN (Shosaku, 1986). These reciprocal excitatory-inhibitory connections between TC and TRN neurons are likely to affect TC spiking, and the information relay from TC to cortex. For instance, large GABAergic conductances from TRN neurons have been shown to diminish information transfer in both computational models (Shosaku, 1986) and hybrid circuits of a model TRN – biological TC pair (Le Masson *et al.*, 2002).

Although TRN neurons are homogeneously GABAergic, the prevailing evidence suggests that intra-TRN inhibition is not prevalent in adult mice (Hou *et al.*, 2016). GABAergic synapses are reported at less than 1% of nearby TRN pairs (Landisman *et al.*, 2002). The dominant source of intra-TRN connectivity, at least between nearby neurons, is thus electrical coupling via connexin36 (Cx36) gap junctions (Landisman *et al.*, 2002). Hence, sensory information relay to cortical neurons from TC neurons is regulated by both GABAergic feedback inhibition from TRN neurons and the electrical synapses between them.

Electrical synapses have been widely reported to participate in the generation of synchronous or phase-locked neuronal activity (Connors & Long, 2004). This role has been confirmed through models of networks with embedded electrical synapses (Lewis & Rinzel, 2003; Pfeuty *et al.*, 2005; Gutierrez *et al.*, 2013). Within thalamocortical circuits, electrical synapses of the TRN help to synchronize the spindle rhythms associated with slow-wave sleep or absence epilepsy (Lewis *et al.*, 2015; Fogerson & Huguenard, 2016). However, the role of electrical synapses in TRN on the transient, stimulus-evoked TC activity is relatively underexplored.

Here we examine the role of electrical synapses within TRN on the activity patterns of TC neurons. We use a reduced model of four cells: two pairs of reciprocally connected TC-TRN neurons, with an electrical synapse between the two TRN neurons. We deliver closely-timed inputs, mimicking inputs of similar temporal, spatial, or frequency arriving from sensory surround, to the TC cells. We examine how TC spiking is impacted by the inhibition delivered from the coupled TRN neurons. Our results demonstrate that electrical synapses can either fuse or further separate input-generate spiking, and we predict that these effects ultimately impacting the ability of recipient cortical cells to discriminate between the inputs.

Methods

Our model is based on a Hogkin Huxley single compartmental models of neurons:

$$C\frac{dV_i}{dt} = (E_{leak} - V_i) \times g_{leak} + \sum_{ion}(E_{ion} - V_i) \times g_{ion}(t) + \sum_{ext}(E_{syn} - V_i) \times g_{syn}(t) +$$

$$\sum_{j \neq i}^{syn}(E_{syn} - V_i) \times g_{syn}(t) + \sum_{j \neq i}(V_j - V_i) \times g_{gap,ji}$$

We used C of 1 μF/cm^2. Ionic currents (g_{bar}, E_{ion}) include fast transient Na^+ current (60.5 mS/cm^2, 50 mV); K^+ delayed rectifier (60 mS/cm^2, -100 mV); K^+ transient A current (5 mS/cm^2, -100 mV); slowly inactivating K-current K2 (0.5 mS/cm^2, -100 mV); slow anomolous rectifier (H current) (0.025 mS/cm^2, -40 mV); low threshold T – Ca^{2+} current (0.67 mS/cm^2, 125 mV); leak current (0.06 mS/cm^2, -75 mV). The membrane voltage initial condition (V_0 = –70.6837 mV) was found by looking for the steady state after a simulation of 5000 ms.

Chemical synapses include fast inhibitory $GABA_A$ (V_{rev} = -75 mV) and excitatory AMPA (V_{rev} = 0 mV) synapses. Synaptic conductance kinetics is implemented with a pair of fall and rise time constants (with $\tau_{rise} = 0.1*\tau_{fall}$ for both synapses); $\tau_{fall,\ GABA}$ = 5 ms and $\tau_{fall,\ AMPA}$ = 2 ms.

$$t_{peak} = \frac{\tau_{fall} \times \tau_{rise}}{\tau_{fall} - \tau_{rise}} \ln \frac{\tau_{fall}}{\tau_{rise}} \; ; f_s = \frac{\tau_{fall}}{-e^{1-\frac{t_{peak}}{\tau_{rise}}} + e^{1-\frac{t_{peak}}{\tau_{fall}}}}$$

$$g(t) = \bar{g} \times (B - A); \frac{dB}{dt} = \frac{B + f_s \times w}{\tau_{fall}}; \frac{dA}{dt} = \frac{A + f_s \times w}{\tau_{rise}}; w = \sum_{spikes} H(t - t_k)$$

$$t_k: time\ of\ event\ k^{th};\ H(x) = \begin{cases} 0\ if\ x < 0 \\ 1\ if\ x \geq 0 \end{cases}$$

Implementation of synapses resembles NEURON's implementation of Traub et al 2005 from ModelDB.

The separation of the spiking windows between TC_1 and TC_2 was also calculated, as the duration between the end of the leading neuron's spiking window and the start of the following neuron's spiking window. In cases of either TC_1 or $_{TC2}$ not spiking, this measure is not calculated. In overlapping cases, this measure is artificially considered to be negative, as loss of separation, and the magnitude is the amount of overlap.

$$\phi_{\text{dur}} = \begin{cases} +\left|\left[\max \sigma_{lead}, \min \sigma_{follow}\right]\right| & if\ \psi = 1\ and\ |\sigma_1| \times |\sigma_2| > 0 \\ -|\sigma_1 \cap \sigma_2| & if\ \psi < 1 \\ NaN & if\ |\sigma_1| \times |\sigma_2| = 0 \end{cases}$$

Our simulated network consists of 2 TRN cells connected via a single electrical synapse, and 2 TC cells receiving external input (Fig. 1A), simulated for 250 ms. Within the network, TRN cells each send inhibitory input to TC cells via $GABA_A$ synapses, and TC cells send excitatory inputs to TRN cells via AMPA synapses. Since the model was easily excitable, no additional DC current was sent to TRN neurons to reach subthreshold excitation. External inputs are excitatory and provided only to the two TC cells.

Electrical synapses (gap junctions) are linear and symmetrical. Values of electrical synapse conductance varied from 0 to 0.025 mS/cm^2, which converts to a coupling coefficient of roughly 0.2883. An applied current, iDC, was used from 0 to – 0.1μA/cm^2 to quantify membrane conductance $g_m \approx 0.0551$ mS/cm^2 and the effective coupling coefficient values, which do not differ significantly with the theoretical values of $g_m/(g_m + g_j)$.

The maximal GABAergic conductance varied from 0 to 0.05 mS/cm^2, and the maximal AMPAergic conductance between TC and TRN cells was fixed at 0.05 mS/cm^2 to make sure that at least two spikes from a TC cell were required to elicit response from a TRN cell. External input to TC_1 stays constant at maximal conductance of 0.06 mS/cm^2, and arrives at 60 ms. The arrival times of external input to TC_2 varied between 10 and 110 ms, with an increment of 10 ms. The maximal conductance of the input to TC_2 varied from 0.02 to 0.1 mS/cm^2. Each simulation was simulated in parallel using MATLAB

R2016 Parallel Toolbox and Lehigh University High Performance Computing Resources (Sol) using ode23.

For each simulation, the number of spikes in each TC neuron was extracted. Separation of spike trains was computed as the time difference between the last spike of the first train and the first spike in the following spike train, and a 5-ms window following each spike was used to allow for EPSP decay in a cortical cell. From each spike train, independence of spike trains was calculated and normalized to values between 0 (complete overlap) and 1 (no overlap) as:

$$Spiking\ Window\ of\ TC_i: \quad \sigma_i = \left[t_i^{(1)}, t_i^{(end)} + 5\right]$$

$$Independence\ of\ TC_i: \quad \psi_i = 1 - \frac{|\sigma_1 \cap \sigma_2|}{|\sigma_i|}$$

$$\psi_i \in [0,1], if\ |\sigma_1|\ or\ |\sigma_2| = 0 \rightarrow\ \psi_1 =\ \psi_2 = 1$$

$$Independence:\ \psi = \sqrt{\frac{\psi_i^2 +\ \psi_2^2}{2}}$$

$$[a,\ b]: Time\ interval\ between\ a,\ b;\ |x|: length\ of\ x$$

Results:

To examine the impact of electrical synapses of the TRN on thalamocortical transmission, we constructed a 4-cell model comprising two pairs of reciprocally connected TC and TRN cells, with an electrical synapse between the two TRN cells (Fig. 1A). Input delivered to TC_1 was fixed at a constant arrival time and strength, and the inputs to TC_2 were varied in arrival time and input strength. To characterize the results of electrical synapses on the output of the TC cells, we quantified independence (ψ) as the percentage as inversely related to the temporal intersection of the two TC spike trains, normalized to the duration of spiking. We also quantified separation (ϕ) as the time interval between the termination of one spike train and the onset of spiking in the other TC cell; negative values of separation result from overlapping trains. Higher values of independence, and positive values of separation, increase the chances that a cortical cell that receives inputs from both of these TC cells will be able to discriminate the input as arising from different pathways (eg whiskers).

With no electrical synapse, the inhibitory feedback from TRN to TC cells is the sole influence that acts to separate the spike trains and thus the inputs that TC relays to cortex (Fig 1B). More specifically, increases in inhibitory strength between TRN and TC cells result in earlier termination of spiking in both TC cells (Fig 1B-D), resulting in both increases in separation and independence of the trains from each other (Fig. 1E).

For increases in strength of the electrical synapse between TRN cells, we observed several effects that ultimately impacted the separation and independence of TC spiking: latency of spiking in the TC that received inputs later, truncation of spike trains, and prevention of any spiking.

An example of GJ-mediated changes in latency is shown in Figure 2. In this case, input was delivered 40 ms to TC_1 before the input in TC_2, and both inputs were of the same strength. Inhibitory strength between TRN and TC cells was relatively low. While the spike trains are always independent in this case, the initial separation (without electrical synapses) is 9.2 ms (Fig. 2A), and a cortical neuron that received inputs from both TC_1 and TC_2 may not differentiate between one spike train that starts 9.2 ms after the termination of the previous. Increases in electrical strength systematically resulted in delayed spiking in TC_2, with corresponding increases in separation, up to 30 ms (Fig. 2A_{iv}), and ultimately prevented spiking in TC_2 (Fig. 2A_{v}). In these cases, separation values follow latencies, and show a strong dependence on both electrical and inhibitory synapse strengths (Fig. 2B), while independence does not vary a great amount. Electrical synapse strength acts synergistically with inhibitory synapse strength (Fig. 2E), such that increases in both parameters result in large latency changes, or ultimately prevention of spiking in TC_2 (whitespace in Fig. 2D).

Spike train truncation arises for stronger values of inhibition in the network. As electrical strength increases, spiking rate in TC_2 decreases (Fig. 3A). Independence of the TC spike trains increases with increases in electrical synapse strength, as the spike train of TC_2 diminishes, and separation also increases (Fig. 3B). For varied values of inhibitory strength within the network, the relationships between independence (Fig 3C), separation (Fig. 3E) and electrical synapses become more complex, as a product of the dependence of rate (Fig. 3D) on both electrical and inhibitory synapse strength.

Rate also depends on the details of the input, specifically on its arrival time and strength. The dependence of spiking rate in TC_2 on electrical and inhibitory synapse strength is shown in Figure 4. Generally, the impacts of electrical synapses between TRN cells are greater for more temporally separated inputs to the TC cells (Fig. 4, top row), as the delays for input integration in TRN cells and the

synaptic delay of inhibition between TRN cells and TC cells determine the timescale at which electrical synapses influence the circuit.

The relationship between electrical and inhibitory synapses, in the context of varied input arrival time and strength, is shown in Figure 5, where identical inputs appear in the center of each subplot, and synapses are varied between panels (cf Fig. 5A). Increases in inhibitory strength generally increase independence, as one would expect, shown by the differences between Fig. 5B through Fig. 5D. Increases in electrical synapse strength, in this context, broaden the set of input differences for which spike trains are independent, seen when comparing panels within Fig. 5B, eg).

Finally, the differences in independence created by electrical synapses are shown in Fig. 6. In this plot, each subpanel is shown as the difference in spike train independence between that set of simulations, and the baseline set of simulations when electrical synapses are absent. From this figure, we see that as electrical synapse strength is increased (left to right), independence of spike trains in the two TC cells can increase or decrease (yellow or blue). It is clear that electrical synapses between TRN neurons add a variety of possible outcomes to TC spike trains, compared to simple feedback inhibition.

Discussion:

Noting that most of the experimental demonstrations or computational simulations of electrical synapses focus on the relationship between electrical synapses and synchrony, we set out to explore the impact of electrical synapses on transient spike train processing within the brain. Using a minimal 4-cell model of paired thalamus and thalamic reticular nucleus cells, with a single electrical synapse to connect the pairs, here we have shown that through feedback inhibition, electrical synapses of the TRN modify both timing and rate of thalamic spiking. Ultimately, the electrical synapses of the TRN modulate both the temporal independence and separation of the spike trains that thalamic cells send on to cortex, thus impacting whether cortical cells receive spike trains that can be discriminated as arising from separate receptors and fields of the sensory surround.

The results of our simulations are important in the context of plasticity of electrical synapses in the TRN (Haas *et al.*, 2011). Our results show that the strength of electrical synapses can shift the character of a network, from one that separates inputs to one that fuses inputs, for instance. Changes in the strength of electrical synapses are represented here by a shift along an axis, and show that even smaller changes in electrical synapse strength have the potential to change output rate, timing, independence and separation.

Our model is the simplest core unit, or motif, of intrathalamic connectivity. However, connections within thalamus and between thalamus and cortex are more complex. Thalamic cells receive convergent inhibitory inputs from multiple TRN cells, and TRN cells receive input from multiple thalamic relay cells. While we have focused on straightforward thalamic relay of singular inputs, mimicking POm, other thalamic subsectors receive inputs from broad areas of the sensory surround. Cortical feedback is also not represented in the present model. Thus, there is much future work to be done to thoroughly explore the role of electrical synapses in transient signal processing within thalamus.

Although our four-cell network is explicitly modeled after thalamus, we expect that its simplicity may allow its results to be extrapolated for cortical signal processing. While connectivity within cortex is much more complex, we expect that the general principles seen here – that electrical synapses act through inhibitory synapses to increase latency, decrease spike rates, and modify the independence of spike trains in principal cells – will hold. In particular, we expect that electrical synapses between retinal A2 amacrine cells may similarly regulate the spike trains produced in retinal ganglion cells,

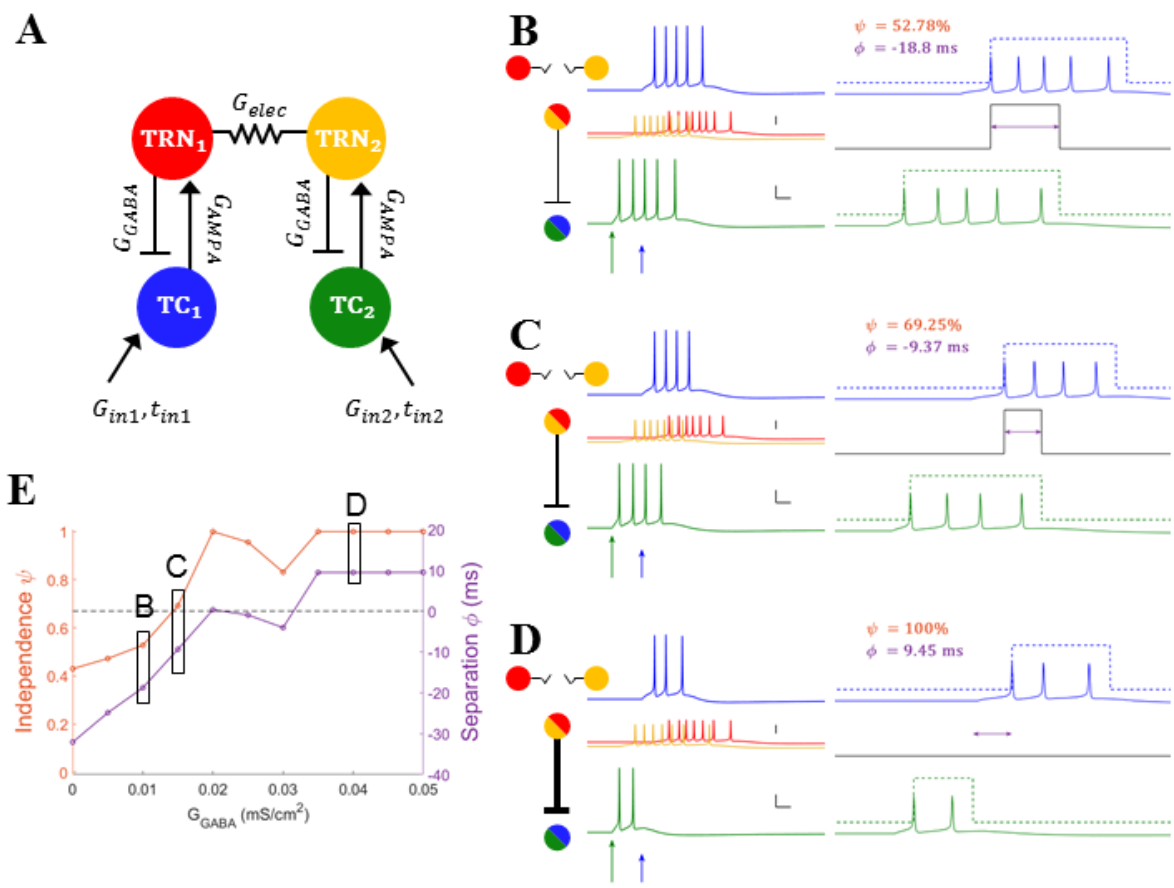

Figure 1. *Model schematic and results with no electrical synapse* **A**: Model is compose of two sets of TRN and TC cells, with reciprocal chemical synaptic connections between pairs, and one electrical synapse between the two TC cells. Each simulation of the model used different values of connection strengths G_{elec}, G_{GABA} and input to TC_2, G_{in2} and t_{in2}. **B, C, D**: Simulation examples, each with $G_{elec} = 0$, and input to TC_2 (green arrow) was large and early ($G_{in2} = 0.09$ mS/cm^2, $t_{in2} = 40$ ms. Input to TC_1 was constant (0.06 mS/cm^2, 60 ms). Over the three simulations shown, inhibitory synapses increased in strength ($G_{GABA} = 0.010$, 0.015, 0.040 mS/cm^2 respectively). In each subpanel, on the left are voltage traces color-coded as in (A), with the TRN traces superimposed and vertically reduced. Scale bars for TC traces are 20 mV, 10 ms; vertical scale bar of TRN traces is 40 mV. TC traces are expanded on the right, to demonstrate the computations for TC independence ψ and separation ϕ. Dotted lines represent the spiking window used to compute independence and separation. The black solid line indicates the amount of temporal overlap of TC spiking windows; purple arrows indicate the amount of temporal separation or overlap. **E**: Independence (orange) and separation (purple) shown for these inputs over all values of G_{GABA}, with letters indicating the examples shown in B, C and D. The dashed black line marks the

transition from overlapping spike trains (negative separation) and completely independent spike trains (positive separation).

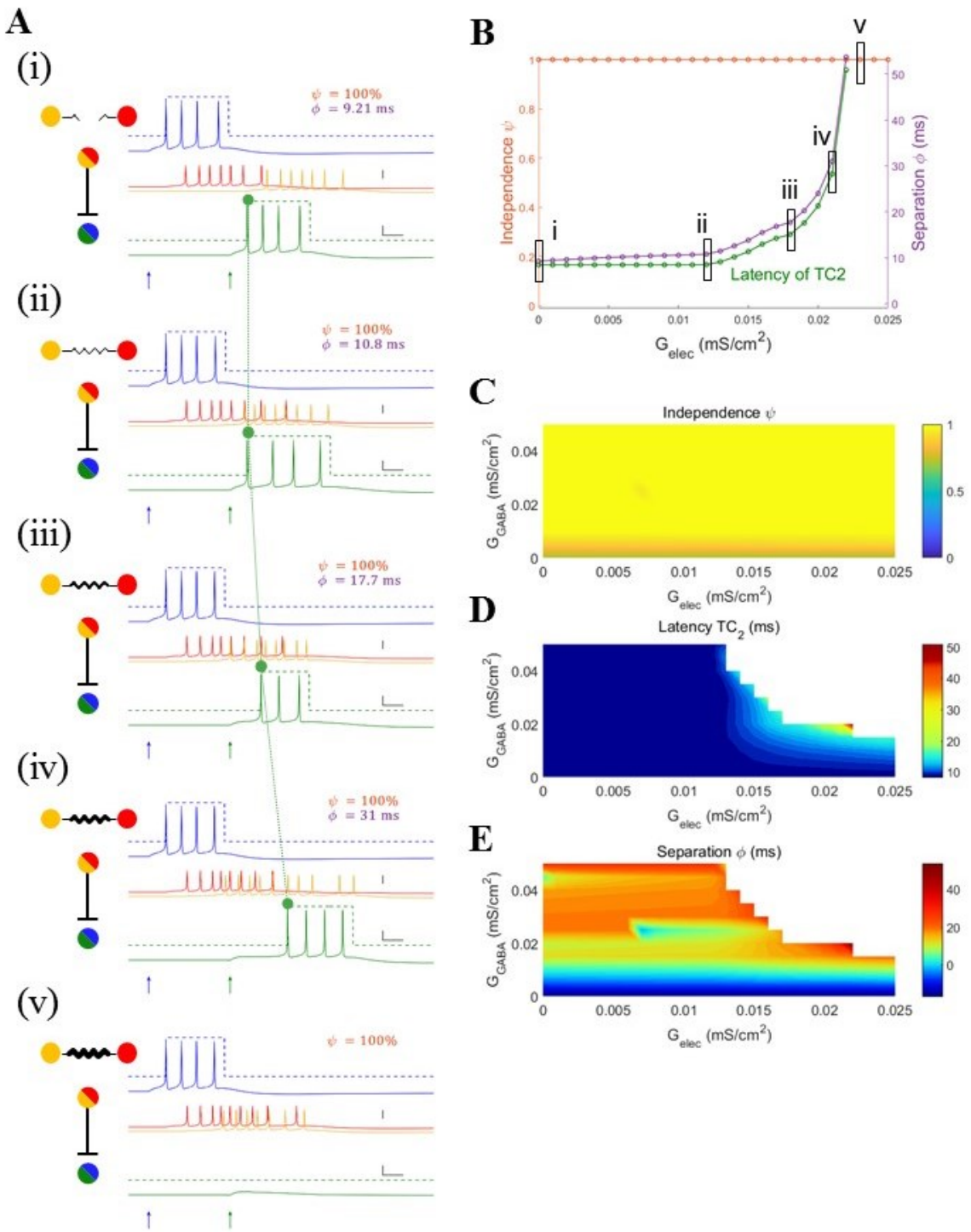

Figure 2. *Electrical synapses between TRN cells result increase latency of TC spiking.*. **A:** Example simulations with superimposed TC spiking windows. Input to TC_1 was constant (0.06 mS/cm^2, 60 ms). For these cases, input to TC_2 was 0.06 mS/cm^2, 100 ms, and inhibitory synapses were G_{GABA} = 0.020

mS/cm^2. Subpanels *i – v* show simulations with increasing electrical synapse strengths (G_{elec} = 0, 0.012, 0.018, 0.021, 0.023 mS/cm^2 respectively); for v, separation is undefined because at least TC_2 does not spike. **B**: Independence (orange), separation (purple) and TC_2 latency (green) for simulations in A, over all values of electrical synapse strength. Latency of TC_2 has the same axis as separation. **C, D, E**: Heat maps for independence, TC_2 latency, separation respectively against G_{elec} and G_{GABA}.

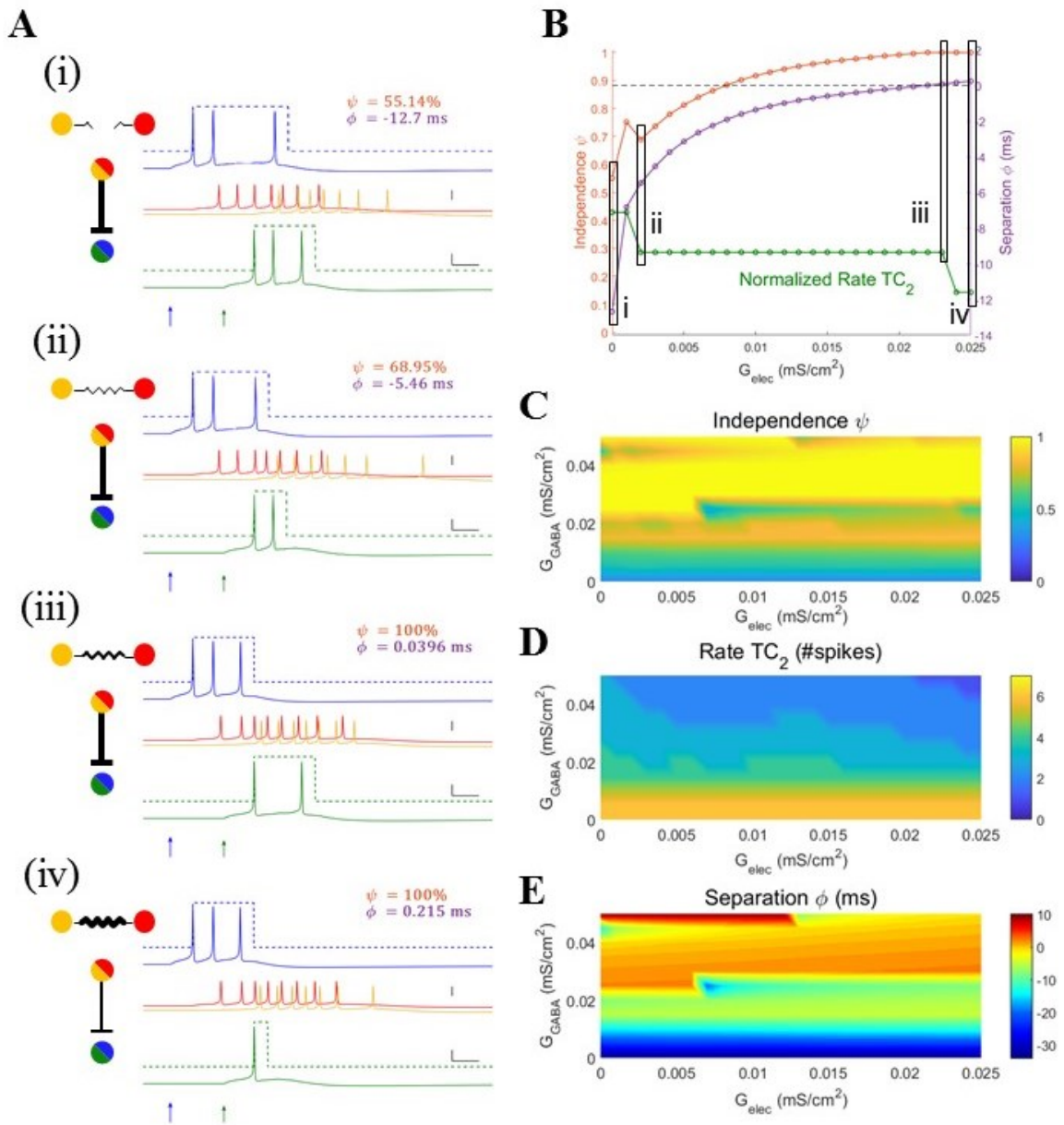

Figure 3. *Electrical synapses between TRN cells result in truncated TC spike trains.* **A**: Example simulated traces. Input to TC_1 was constant (0.06 mS/cm^2, 60 ms). For these cases, input to TC_2 was 0.05 mS/cm^2, 80 ms and inhibitory synapses were G_{GABA} = 0.045 mS/cm^2; Subpanels *i – v* show simulations with increasing electrical synapse strengths (G_{elec} = 0, 0.002, 0.023, 0.025 respectively). **B**: Independence (orange), separation (purple) and normalized TC_2 rate (green) for the set of simulations in (A) plotted against electrical synapse strength. Normalized rate of TC_2 is the number of TC_2 spikes relative to the

maximum over all simulations (7 spikes). **C, D, E**: Heat map for independence, TC_2 rate (unnormalized), and separation respectively plotted against G_{elec} and G_{GABA}.

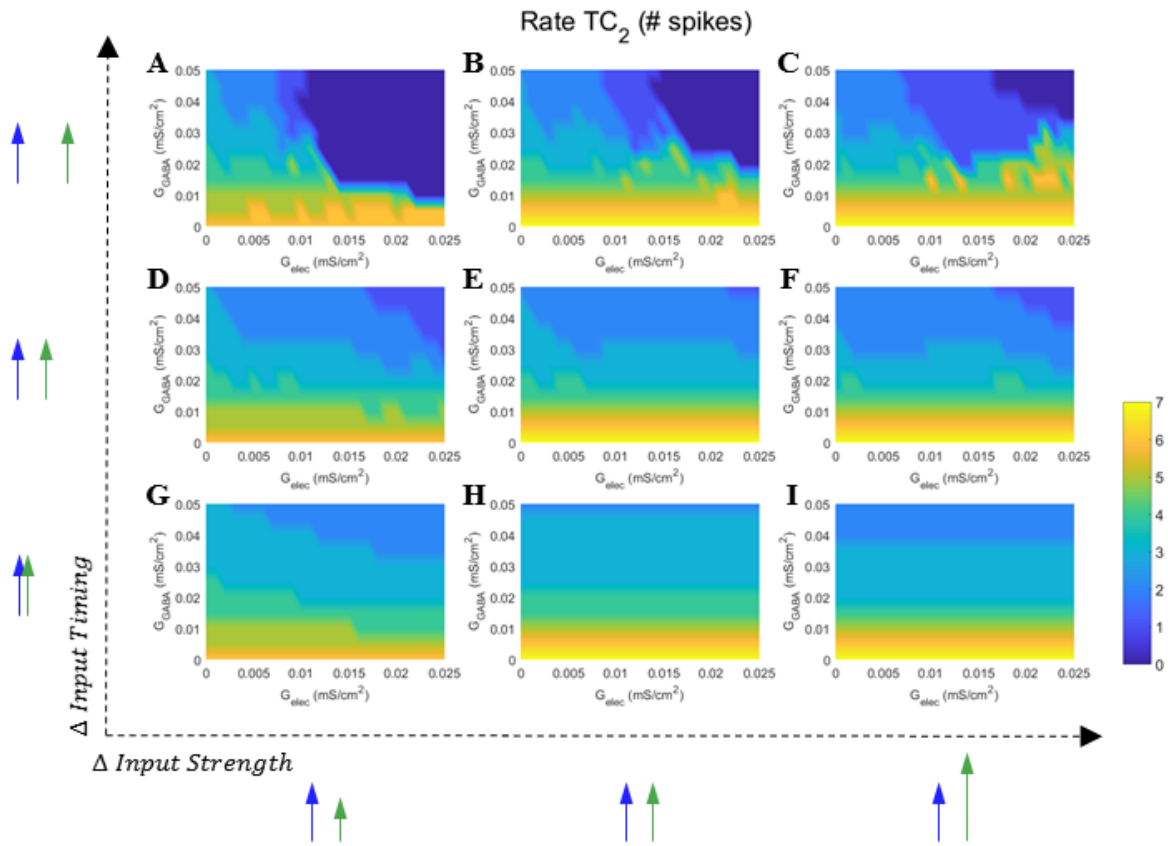

Figure 4. *Electrical synapses between TRN cells modulate rate of TC_2.* Each panel (**A – I**) is a heat map for TC_2 rate, plotted against all values of G_{elec} and G_{GABA}. Input strengths to TC_2 were varied between panels from left to right (0.04, 0.06 and 0.08 mS/cm^2; input to TC_1 was always 0.06 mS/cm^2), and input timing was varied from bottom to top (tin1 = 60, 80 and 100 ms; t_{in1} was always 60 ms).

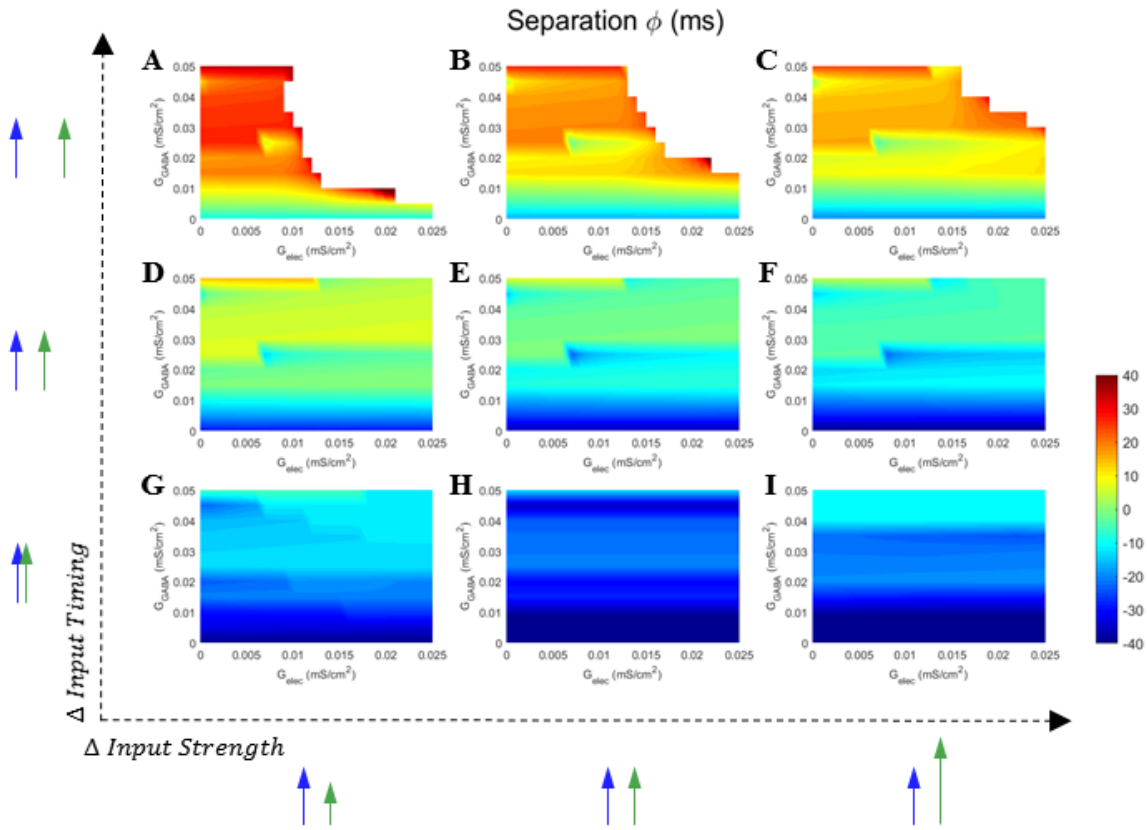

Figure 5. *Electrical synapses between TRN cells increase separation of TC spike trains*. Each panel (**A – I**) is a heat map for separation between TC spike trains, plotted against all values of G_{elec} and G_{GABA}. Input strengths to TC_2 were varied between panels from left to right (0.04, 0.06 and 0.08 mS/cm^2; input to TC_1 was always 0.06 mS/cm^2), and input timing was varied from bottom to top (tin1 = 60, 80 and 100 ms; t_{in1} was always 60 ms).

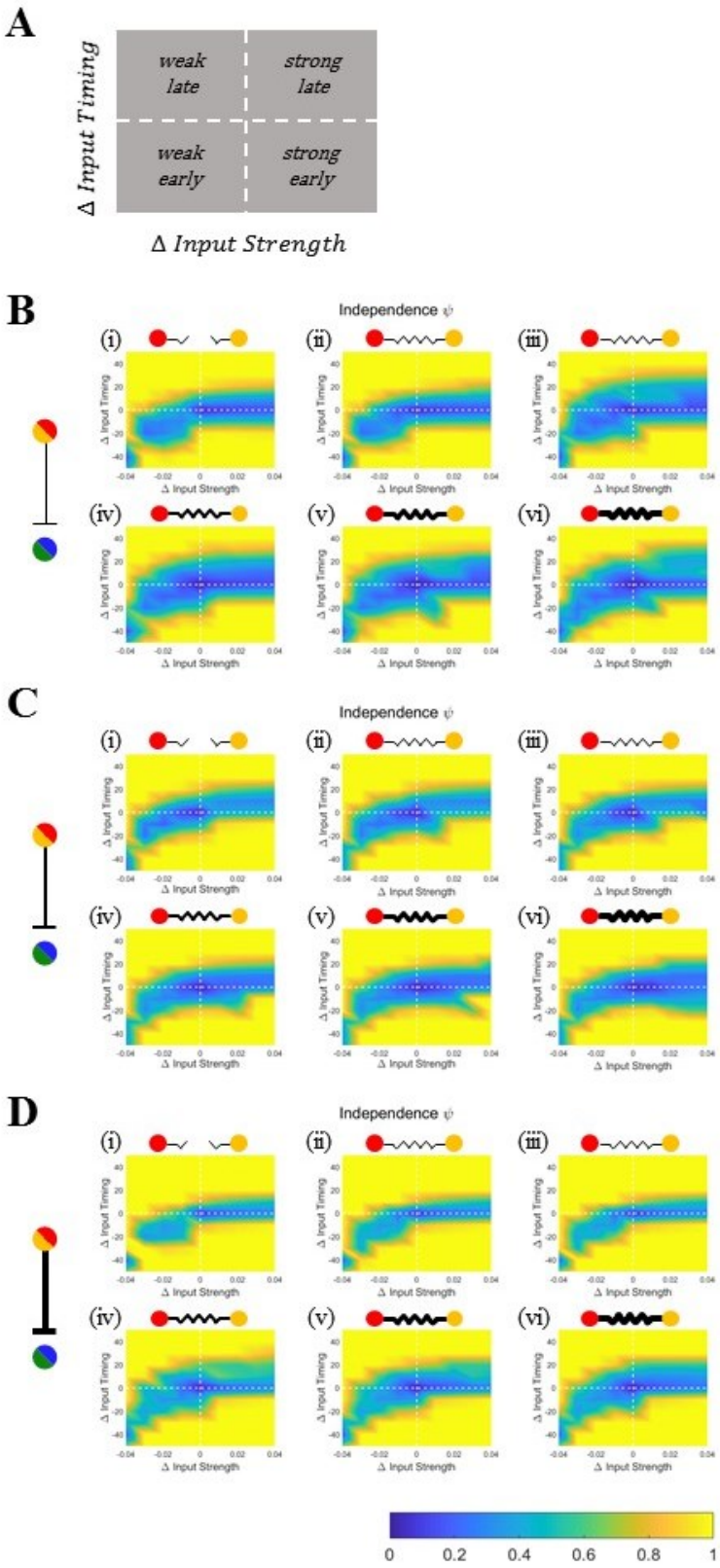
A
weak late
strong late
weak early
strong early
Δ Input Timing
Δ Input Strength
B
C
D
Independence ψ
(i)
(ii)
(iii)
(iv)
(v)
(vi)
Δ Input Timing
Δ Input Strength
0
0.2
0.4
0.6
0.8
1

Figure 6. *Electrical synapses between TRN cells merge TC spike trains for inputs that are similar in timing and strength.* **A**: Display convention for the following results, plotted by the differences of inputs to TC_2 in arrival time and strength relative to the fixed input to TC_1. The horizontal and vertical dashed lines represent simultaneous and equal inputs, respectively. **B, C, D**: Independence plotted for varied values of electrical synapse strength and GABAergic inhibition (G_{GABA} = 0.025 in **B**, 0.040 in **C**, 0.050 mS/cm^2 in **D**). The electrical synapse strength is indicated by thickness of symbol (G_{elec} = 0, 0.005, 0.010, 0.015, 0.020, 0.025 mS/cm^2).

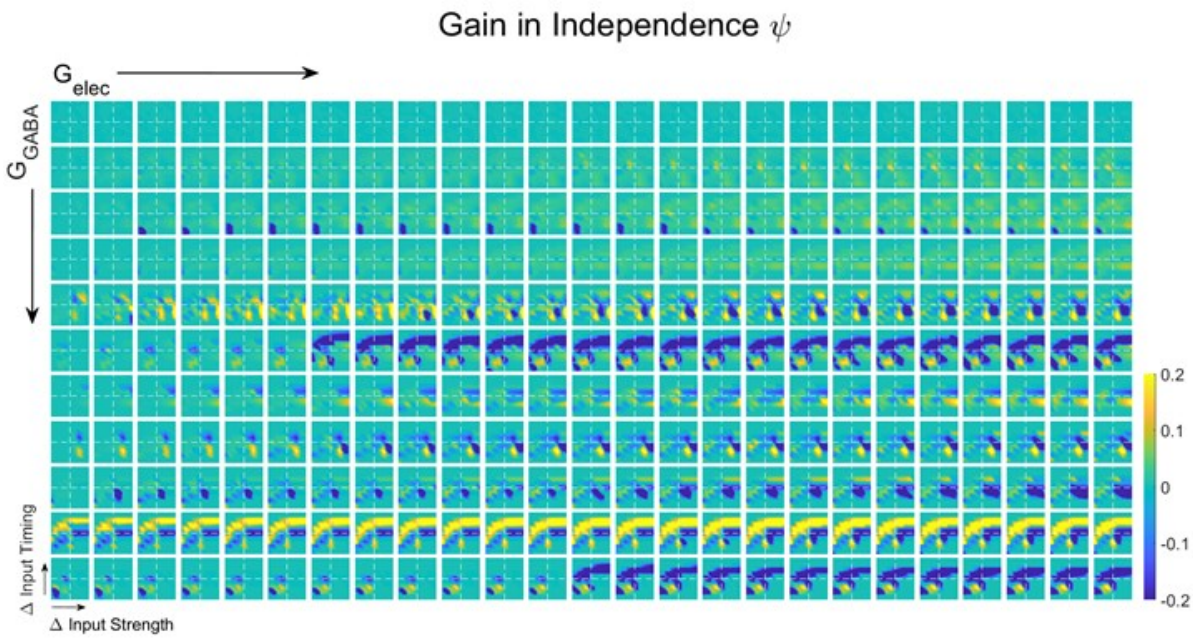

Figure 7. *Change in TC spiking independence, compared to unconnected (G_{elec} = 0) baseline, resulting from electrical synapses between TRN cells.* Each subpanel is the difference of TC spike train independence, between the presence of electrical synapse and the unconnected case with similar inhibitory conductance. Within each subpanel, input strength and size are represented as in Figure 6, with horizontal and vertical dashed lines representing simultaneous and equal inputs, respectively. From left to right, electrical synapse conductance increases across panels (G_{elec} = 0.001 to 0.025 mS/cm^2). From top to bottom, inhibitory synapse conductance increases (G_{GABA} = 0 to 0.050 mS/cm^2).

References

Alloway KD. (2008). Information processing streams in rodent barrel cortex: the differential functions of barrel and septal circuits. *Cereb Cortex* **18,** 979-989.

Connors BW & Long MA. (2004). Electrical synapses in the mammalian brain. *Annu Rev Neurosci* **27,** 393-418.

Fogerson PM & Huguenard JR. (2016). Tapping the Brakes: Cellular and Synaptic Mechanisms that Regulate Thalamic Oscillations. *Neuron* **92,** 687-704.

Gutierrez GJ, O'Leary T & Marder E. (2013). Multiple mechanisms switch an electrically coupled, synaptically inhibited neuron between competing rhythmic oscillators. *Neuron* **77,** 845-858.

Haas JS, Zavala B & Landisman CE. (2011). Activity-dependent long-term depression of electrical synapses. *Science* **334,** 389-393.

Hou G, Smith AG & Zhang ZW. (2016). Lack of Intrinsic GABAergic Connections in the Thalamic Reticular Nucleus of the Mouse. *J Neurosci* **36,** 7246-7252.

Houser CR, Vaughn JE, Barber RP & Roberts E. (1980). GABA neurons are the major cell type of the nucleus reticularis thalami. *Brain Res* **200,** 341-354.

Landisman CE, Long MA, Beierlein M, Deans MR, Paul DL & Connors BW. (2002). Electrical synapses in the thalamic reticular nucleus. *J Neurosci* **22,** 1002-1009.

Le Masson G, Renaud-Le Masson S, Debay D & Bal T. (2002). Feedback inhibition controls spike transfer in hybrid thalamic circuits. *Nature* **417,** 854-858.

Lewis LD, Voigts J, Flores FJ, Schmitt LI, Wilson MA, Halassa MM & Brown EN. (2015). Thalamic reticular nucleus induces fast and local modulation of arousal state. *Elife* **4,** e08760.

Lewis TJ & Rinzel J. (2003). Dynamics of spiking neurons connected by both inhibitory and electrical coupling. *J Comput Neurosci* **14,** 283-309.

Pfeuty B, Mato G, Golomb D & Hansel D. (2005). The combined effects of inhibitory and electrical synapses in synchrony. *Neural Comput* **17,** 633-670.

Shosaku A. (1986). Cross-correlation analysis of a recurrent inhibitory circuit in the rat thalamus. *J Neurophysiol* **55,** 1030-1043.

Sosnik R, Haidarliu S & Ahissar E. (2001). Temporal frequency of whisker movement. I. Representations in brain stem and thalamus. *J Neurophysiol* **86,** 339-353.

Yu C, Horev G, Rubin N, Derdikman D, Haidarliu S & Ahissar E. (2015). Coding of object location in the vibrissal thalamocortical system. *Cereb Cortex* **25,** 563-577.